EKF BASED LOCALIZATION ALGORITHM FOR LOS AND MULTIPATH

A Project Report

submitted by

N CHANDRASEKHAR

(EE09B011)

in partial fulfilment of the requirements
for the award of the degree of

BACHELOR OF TECHNOLOGY
in
ELECTRICAL ENGINEERING

DEPARTMENT OF ELECTRICAL ENGINEERING
INDIAN INSTITUTE OF TECHNOLOGY, MADRAS.

MAY 2013

PROJECT CERTIFICATE

This is to certify that the project titled **EKF BASED LOCALIZATION ALGORITHM FOR LOS AND MULTIPATH**, submitted by **N Chandrasekhar (EE09B011)**, to the Indian Institute of Technology, Madras, for the award of the degree of **Bachelor of Technology**, is a bona fide record of the project work done by him under my supervision. The contents of this report, in full or in parts, have not been submitted to any other Institute or University for the award of any degree or diploma.

Prof. Devendra Jalihal
Project Guide
Professor
Dept. of Electrical Engineering
IIT Madras, Chennai 600 036

Prof. Enakshi Bhattacharya
Head
Dept. of Electrical Engineering
IIT Madras, Chennai 600 036

Place: Chennai

Date: May 16, 2013

ACKNOWLEDGEMENTS

I would like to thank Prof. Devendra Jalihal for his valuable guidance and support without which this work would not have been possible. I would like to express thanks to Mr Ishtadev, a Phd scholar for agreeing to help me at any time. I am grateful to my family and friends at IIT Madras for their constant motivation, encouragement and support.

ABSTRACT

KEYWORDS: Multilateration ; $TDOA$; Extended Kalman Filtering; Multipath channel.

Extended Kalman Filtering is a recursive algorithm for estimation in a non-linear process and measurement model. In this thesis, an algorithm is proposed employing the multilateration technique for Mobile Station (MS) localization. First, the performance of the algorithm along with several other attributes are studied for two different mobility models for an LOS environment. This is followed by a performance study in a multipath environment with pre-defined channel characteristics determined by the Jake's model and different Power Delay Profiles.

TABLE OF CONTENTS

LIST OF TABLES

LIST OF FIGURES

ABBREVIATIONS

MS	Mobile Station
BS	Base Station
TOA	Time of Arrival
$TDOA$	Time Difference of Arrival
AOA	Angle of Arrival
$RSSI$	Received Signal Strength Indication
EKF	Extended Kalman Filtering
PDP	Power Delay Profile

CHAPTER 1

INTRODUCTION

A general outline of the problem statement and the thesis is described in this section.

1.1 Background

Localization is the pinpointing of the position of an object on the surface of the Earth, and is measured in terms of latitude and longitude. This thesis concerns MS (Mobile Station) localization. The MS transmits and receives signals to and from various BS (Base Stations). Various aspects of these signals could be used for pinpointing MS location to varying degrees of accuracy. For example, TOA (Time of Arrival) data could be employed. However, the problem involves factors like how the MS moves (the mobility model), noise present in data and so on. Algorithms or pinpointing could be static, like the least squares method or recursive, like Kalman Filtering. We try to develop an algorithm based on Extended Kalman Filtering for localization, and study its performance aspects under various scenarios.

1.2 Problem Statement

Consider an environment with a pre-set number of base stations (BS) at specified locations in a 2×2 grid. The problem is to come up with an accurate and reliable algorithm for mobile phone tracking in various environments and mobility models, and check performance. The algorithm must employ the multilateration technique to overcome the synchronization problem faced in trilateration. It has to be tested for robustness with respect to varying measurement

error and the complexity aimed to be minimized. It has to be simulated for two realistic multipath channel to check performance.

1.3 Thesis outline

In Chapter 2, different kinds of localization schemes are introduced. Various measurements which are useful in solving the localization problem are investigated. A few localization algorithms available in literature are also mentioned. In Chapter 3, the concept of Extended Kalman Filtering is introduced in context with localization. Simulations, results and conclusions are discussed in Chapter 4.

CHAPTER 2

Localization techniques

2.1 Trilateration

Trilateration is the fundamental concept behind most localization algorithms. It is a method to determine the position of an object based on simultaneous range measurements from three or more known locations (the locations being non-collinear). In 2D geometry, it is known that if a point lies on two curves such as the boundaries of two circles then the circle centres and the two radii provide sufficient information to narrow the possible locations down to two. Additional information may narrow the possibilities down to one unique location. It could employ TOA data, which are described subsequently in the chapter. [1] employs trilateration for localization.

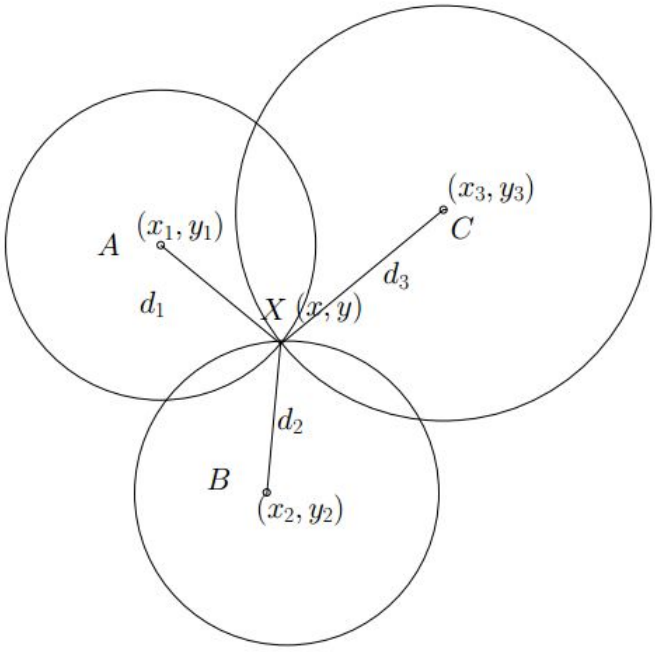

Figure 2.1.1: Trilateration

2.2 Multilateration

Multilateration is a technique based on the measurement of the difference in distance to two or more stations at known locations that broadcast signals at known times. Difference in distance gives a hyperbolic locus for the object in 2D. With two or more sites, the object is fully localized. Multilateration could employ $TDOA$ data, described later in the chapter. This thesis employs Multilateration for localization. Acquiring absolute time values as in trilateration is difficult and more error prone as compared to obtaining difference in arrival time from the MS point of view.

2.3 Subspace based approaches

They are linear methods for noise reduction. Information is contained in a small linear subspace of the possible sample vectors (signals), whereas additive noise is distributed isotropically. A subspace based localization algorithm is discussed in [2].

2.4 Metrics in localization algorithms

The most common metrics associated with the localization process are discussed in this section.

2.4.1 TOA (Time of Arrival)

These measurements involve the travel time of a radio signal from a single transmitter to a remote single receiver. By the relation between light speed in vacuum and the carrier frequency of a signal the time is a measure for the distance between transmitter and receiver. TOA uses the absolute time of arrival at a certain base station. For this technique to work properly we need the

receiver and transmitter clocks to be synchronized. The need for highly synchronized clocks places a heavy burden on the equipment cost.

A lot of factors such as humidity, temperature etc affect speed of propagation of ultrasound signals and therefore, Radio Frequency signals are used in general. Multipath signals also affect localization that employ TOA data.

2.4.2 $TDOA$ (Time Difference of Arrival)

$TDOA$ measurements involve the difference in the travel time of a radio signal from two transmitters to a remote single receiver. This overcomes the synchronization problem faced in the TOA scenario as the difference in arrival times is measured.

The technique has various ways of implementation, but in this thesis, the $TDOA$ values for two base stations from a single MS are considered. This gives a hyperbolic locus for the location of the MS with the two base stations as the foci. With more such values, the MS can be localized.

2.4.3 AOA (Angle of Arrival)

AOA measurement is a method for determining the direction of propagation of a radio-frequency wave incident on an antenna array. Direction is determined by measuring the $TDOA$ at individual elements of the array from which AOA can be calculated. An algorithm based on AOA is proposed in [3].

This technique is least popular due to high sensitivity to multipath signals and high costs involved.

2.4.4 $RSSI$ (Received Signal Strength Indication)

Radio Frequency signals attenuate as they move through space. $RSSI$ is an indication of the power level being received by the antenna. Distance between source and receiver can be calculated using received signal strength, the transmitted power and a path loss model for the channel.

CHAPTER 3

Algorithm for Localization

In this section Extended Kalman Filtering is applied to the localization process using the multilateration technique. The state transition model and measurement model are described for the localization problem and an algorithm is proposed.

3.1 State and measurement model for multilateration

The EKF algorithm is an extension of the linear Kalman filter. The latter assumes the state transition and measurement to be linear models. An algorithm for localization based on Kalman filtering is described in [4] and [5]. EKF, however, relaxes the linearity assumption of the Kalman filter. The state equation could be the following:

$$s(k) = f(s(k-1)) + w(k) \tag{3.1}$$

where $s(k)$ refers to the state and $w(k)$ is zero mean multivariate Gaussian process noise with covariance $Q(k)$. The function f is differentiable and can be used to calculate the predicted state from the previous estimate.

Similarly, the measurement equation could be as follows:

$$z(k) = h(x(k)) + v(k) \tag{3.2}$$

where $z(k)$ is the observation vector and $v(k)$ is zero mean uncorrelated measurement noise with covariance $R(k)$. The function h is differentiable and can compute predicted measurement from predicted state.

The localization problem based on multilateration can be described in this formulation in the following way, from [4]. In a two dimensional scenario, if the location of the object $s(k) = [x(k), y(k), v_x(k), v_y(k)]^T$ is defined as the state of the object. The state model considered involves the following state transition equation.

$$s(k+1) = Ts(k) + w(k) \tag{3.3}$$

$s(k)$ and $w(k)$ areas defined before. T is the following matrix.

$$T = \begin{bmatrix} 1 & 0 & \Delta & 0 \\ 0 & 1 & 0 & \Delta \\ 0 & 0 & 1 & 0 \\ 0 & 0 & 0 & 1 \end{bmatrix} \tag{3.4}$$

Δ is the time interval between samples. We observe that the measurement equation is linear. The measurement equation, however, is non-linear. The proposed algorithm is based on $TDOA$ of signals from the MS to various BS. By multiplication with c these are converted to range (distance) differences of the MS from various BS. If (x_i, y_i) refers the position of BS number i in the two dimensional environment, and r_{ij} refers to the difference of distance from BS number i to j of the MS, we obtain the following measurement equation.

$$r_{ij} = \sqrt{(x_i - x(k))^2 + (y_i - y(k))^2} - \sqrt{(x_j - x(k))^2 + (y_j - y(k))^2} + v \tag{3.5}$$

There could be as much as $\binom{N}{2}$ values of r_{ij} that could figure in the measurement model. For a two dimensional scenario three are sufficient for localization. The R.H.S of (3.5) includes v, which is Gaussian measurement noise. We assume that the measurement noises are uncorrelated with one another. Thus the measurement equation is formed as a non-linear equation involving the state variables.

3.2 Prediction and Update

The predict and update equations for EKF are described here, from [6], describing them on the basis of of Equations (3.1) and (3.2).

3.2.1 Prediction

Predicted state estimate:

$$\hat{s}(k|k-1) = f(\hat{s}(k-1|k-1)) \tag{3.6}$$

$\hat{s}(k|k-1)$ is the predicted state at iteration k based on the previous $k-1$ measurement data.
Predicted covariance estimate:

$$P(k|k-1) = F(k-1)P(k-1|k-1)F^T(k-1) + Q(k-1) \tag{3.7}$$

$F(k-1)$ is $\frac{\partial f}{\partial s}$ evaluated at $\hat{s}(k-1|k-1)$.

3.2.2 Update

Innovation:

$$\tilde{y}(k) = z(k) - h(\hat{s}(k|k-1) \tag{3.8}$$

Innovation covariance:

$$S(k) = H(k)P(k|k-1)H^T(k) + R(k) \tag{3.9}$$

Kalman gain:

$$K(k) = P(k|k-1)H^T(k)S^{-1}(k) \tag{3.10}$$

Updated state estimate:

$$\hat{s}(k|k) = \hat{s}(k|k-1) + K(k)\tilde{y}(k) \tag{3.11}$$

Updated estimate covariance

$$P(k|k) = (I - K(k)H(k))P(k|k-1) \tag{3.12}$$

$H(k)$ is $\frac{\partial h}{\partial s}$ evaluated at $\hat{s}(k-1|k-1)$, I is the identity matrix.

We use the state transition model and measurement model suggested in Equations (3.3) and (3.5) in concordance with the prediction and update presented in section 3.2.2 to generate the algorithm.

CHAPTER 4

Simulation, Results and Conclusions

This section demonstrates the mobility models and the algorithm performance for both an LOS and a multipath environment.

4.1 Velocity perturbation mobility model

The first mobility model assumes a constant velocity for the object, perturbed by mild variations of the environment such as wind gusts, slight speed corrections and so on. These perturbations are modelled as noise additions to the velocity, and are assumed to be normally distributed and uncorrelated with each other. The model, therefore takes the following form:

$$v_x[n] = v_x[n-1] + u_x[n] \tag{4.1}$$

Similarly for the y direction,

$$v_y[n] = v_y[n-1] + u_y[n] \tag{4.2}$$

$v_x[n]$ and $v_y[n]$ denote the x and y components of velocities respectively. $u_x[n]$ and $u_y[n]$ are the noise perturbations. Also

$$r_x[n] = r_x[n-1] + v_x[n-1]\Delta \tag{4.3}$$

Similarly for the y direction,

$$r_y[n] = r_y[n-1] + v_y[n-1]\Delta \tag{4.4}$$

$r_x[n]$ and $r_y[n]$ denote the x and y components of position respectively. This

simulation involves the following parameters with their corresponding values:

S.no	Parameter	Value
1	Δ (Time step duration)	$0.01s$
2	Perturbation variance	0.01
3	Velocity of MS	$1m/s$

Table 4.1: Parameter values 1

Without perturbations, the velocities would be constant and the vehicle would move in a straight line, as indicated by the red lines in Figure 4.1.1 . The blue line indicates the path of the vehicle with perturbations in velocity. The number of time steps (iterations) is 30. However as time increases, the true trajectory gradually deviates from the straight line path in this model as shown in Figure 4.1.2 , for 100 iterations.

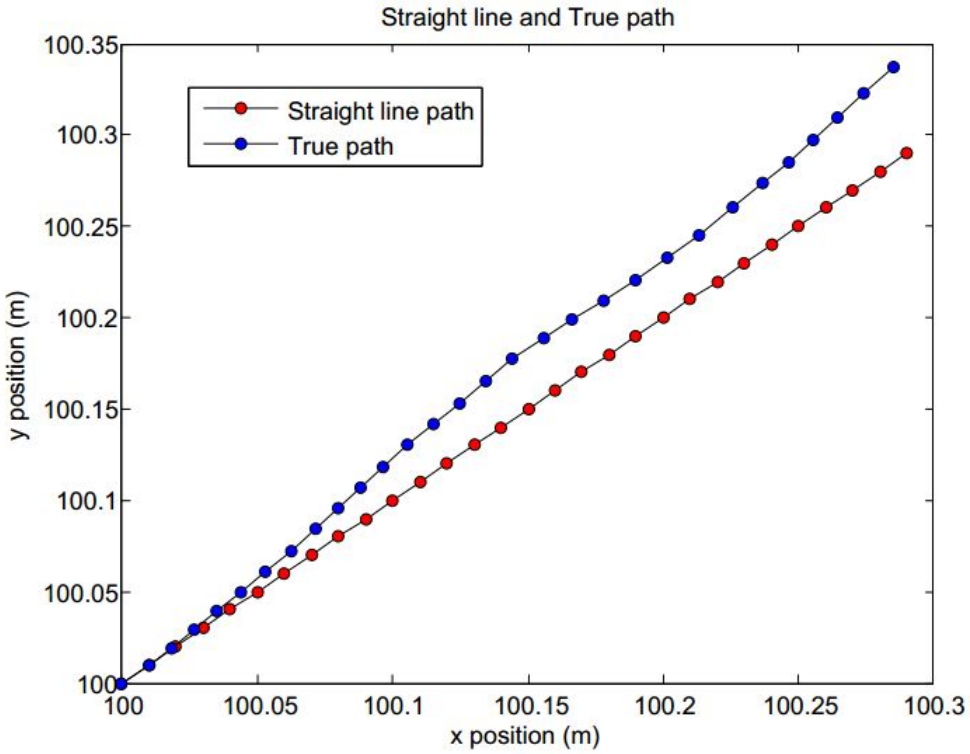

Figure 4.1.1: Few iterations

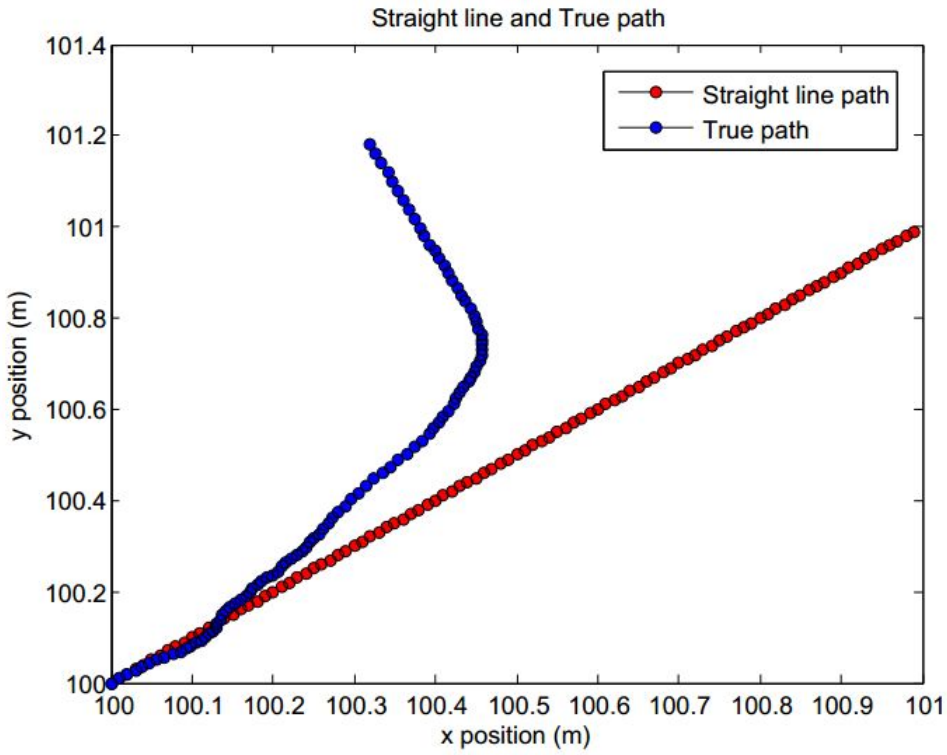

Figure 4.1.2: Large number of iterations

The unboundedness of $r_x[n]$ and $r_y[n]$ is as a result of the variances of $v_x[n]$ and $v_y[n]$ eventually increasing to infinity. The proof of that is outside the scope of this thesis.

4.1.1 Algorithm performance for mobility model 1

The performance of the algorithm is expressed as a plot of

$$e_n = \sqrt{(x_n - \tilde{x_n})^2 + (y_n - \tilde{y}_n)^2} \tag{4.5}$$

versus n, where (x_n, y_n) is the actual position of the MS known to the simulator, $(\tilde{x}_n, \tilde{y}_n)$ is the estimated MS position and $'n'$ is the time index. This criteria of performance is followed throughout this thesis.

The base station configuration employed for the first performance simulation is depicted in Figure 4.1.3.

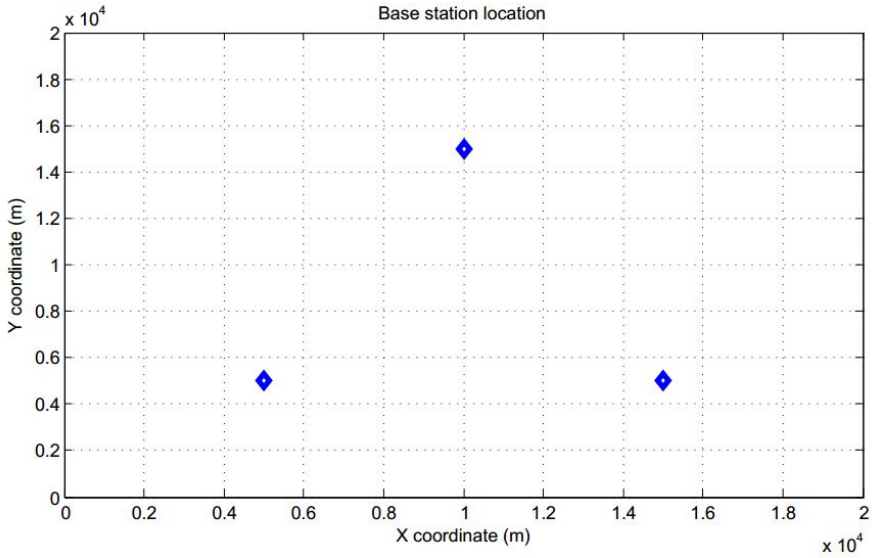

Figure 4.1.3: BS configuration 1

The algorithm performance is shown in Figure 4.1.4. It is not, however an accurate depiction of the error as the position diverges significantly from the straight line path as mentioned before. Therefore, the values obtained as inputs to the EKF would change significantly.

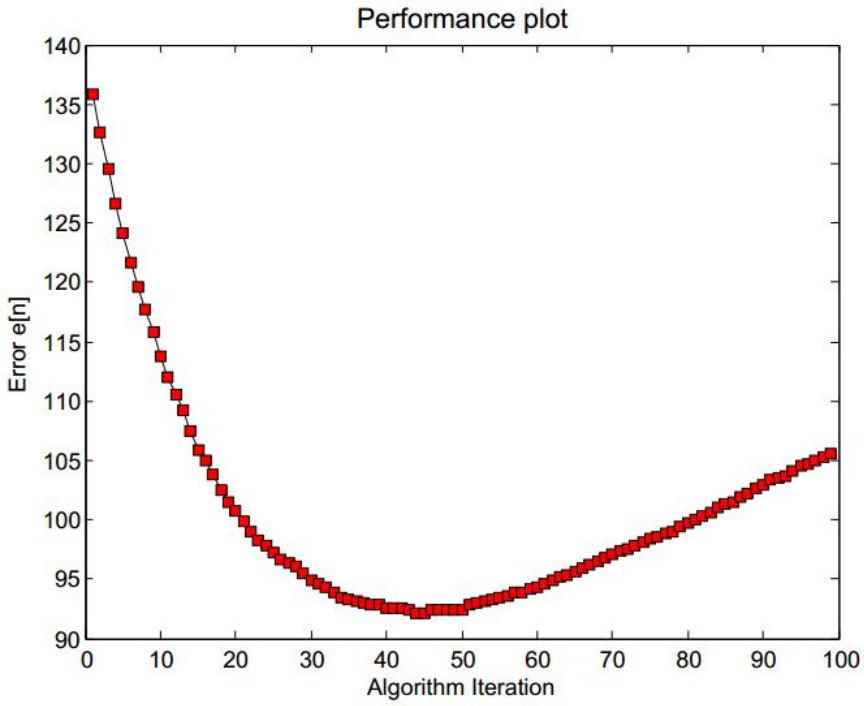

Figure 4.1.4: Algorithm performance for model 1

4.2 Random walk model

In this model, we assume that the MS at an arbitrary (x, y) takes random steps towards $(x-1, y-1)$, $(x-1, y+1)$, $(x+1, y-1)$ or $(x+1, y+1)$ with equal probability. This is shown in Figure 4.2.1.

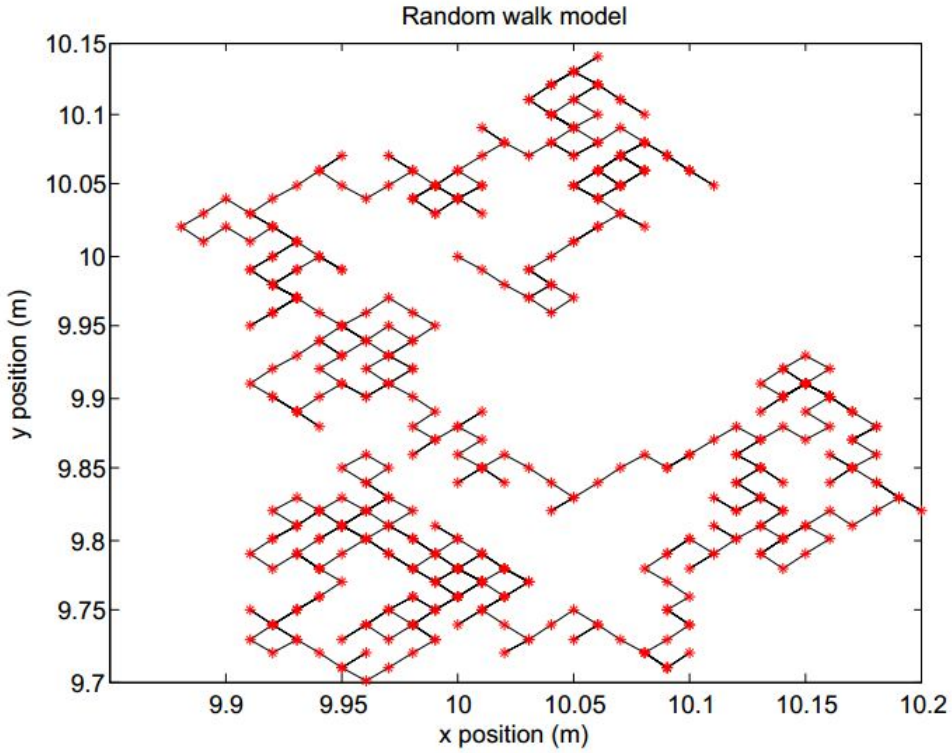

Figure 4.2.1: The random walk model

4.2.1 Performance with measurement error

In this subsection, the algorithm is simulated for a simple case of BS configuration as in Figure 4.1.3 for different measurement error values. Noise is dependent on how large the range difference actually is, in the sense that the simulation adds noise proportional to the actual measurement value. To construct the measurement matrix, noise variance for each measurement is made proportional to the actual measurement value. Base stations farther away would generate larger noise, and the above is an attempt to capture that fact. Therefore, as the MS moves, different values of the time-differences (converted to

range-differences by multiplication with the speed of light factor) are perceived depending on distances from the base stations.

The parameters involved in this simulation are shown in the table below:

S.no	Parameter	Value
1	Δ (Time step duration)	$0.01s$
2	Initial MS position	$(10, 10)$
3	Velocity of MS	$1m/s$

Table 4.2: Parameter values 2

We observe that all three towers are roughly equally spaced from the MS for a significant number of iterations or time steps, for the configuration shown in Figure 4.1.3, and for a mobility model similar to the one in Figure 4.1.5, where the MS does not deviate very much from the initial point. The error for all three range differences, thus, would be roughly of the same magnitude throughout the simulation. The algorithm is run for low error, medium error and high error in this simulation environment.

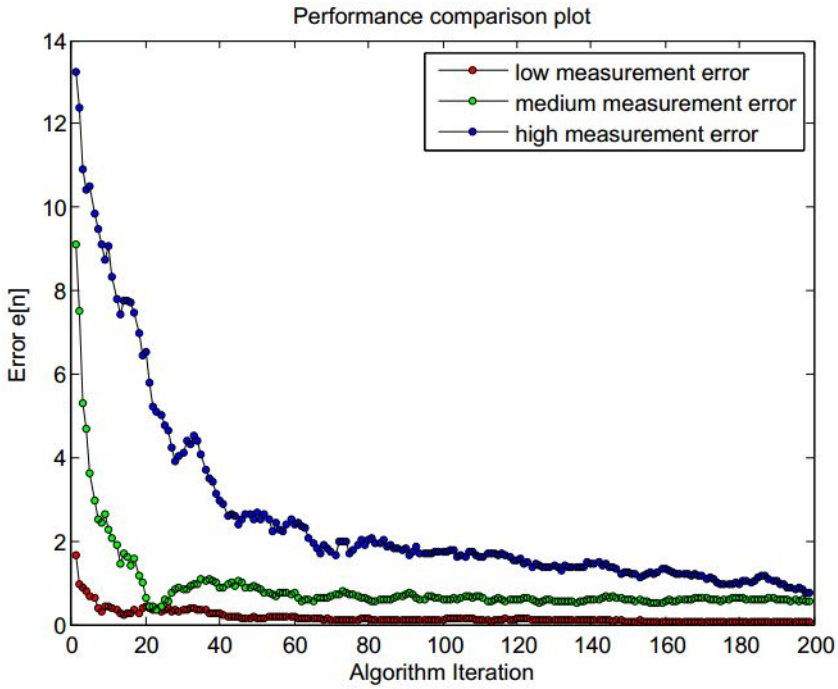

Figure 4.2.2: Plots for different measurement errors

We see from Figure 4.2.2 that the algorithm is robust, and converges for different magnitudes of error quite rapidly. This is further shown in Figure 4.2.3, where the difference in the iteration error (4.5) is plotted for the various pairs of the test cases involved in the previous case versus $'n'$, the iteration number. We see that all three plots converge to zero quite rapidly.

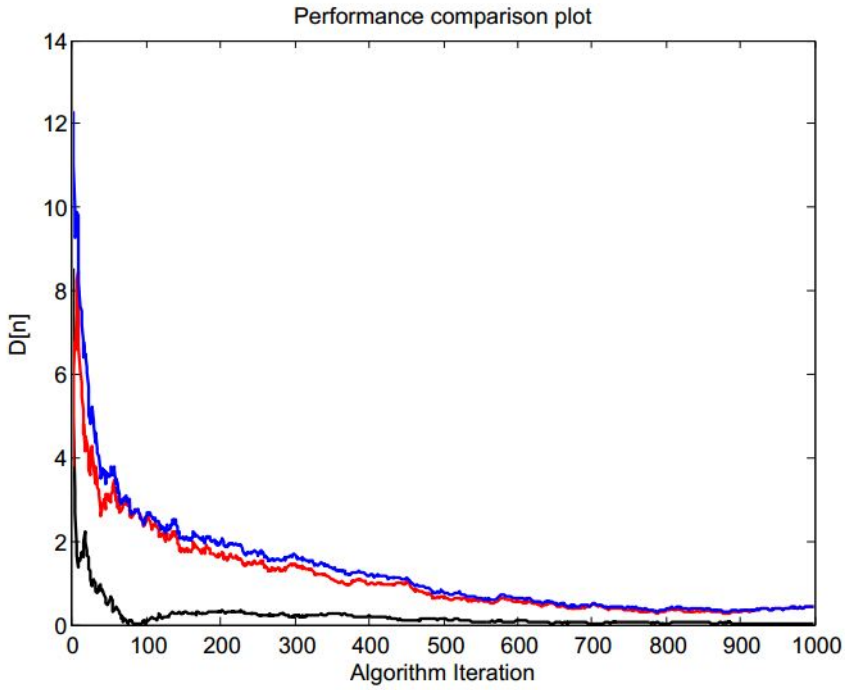

Figure 4.2.3: Illustration of algorithm robustness

4.2.2 Measurement inputs

In this subsection, an analysis of the effect of number of measurement inputs versus algorithm performance is done for varying number of BS, BS configurations and measurement errors. The computational complexity of the algorithm varies according to the number of base stations taken into consideration. Therefore, lesser base stations would lead to a computationally simpler algorithm, though we need to analyze how performance is affected.

We first consider 6 base stations in a circle as shown in Figure 4.2.4. The

simulation is run taking 3, 4, 5, and finally all 6 BS into consideration.

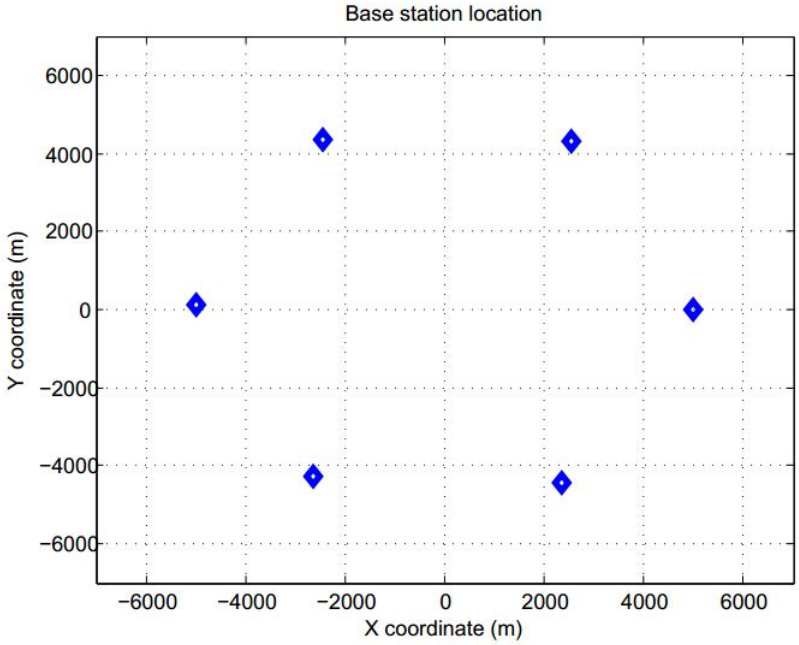

Figure 4.2.4: BS configuration 2

The algorithm is then simulated for low measurement error and high measurement error.

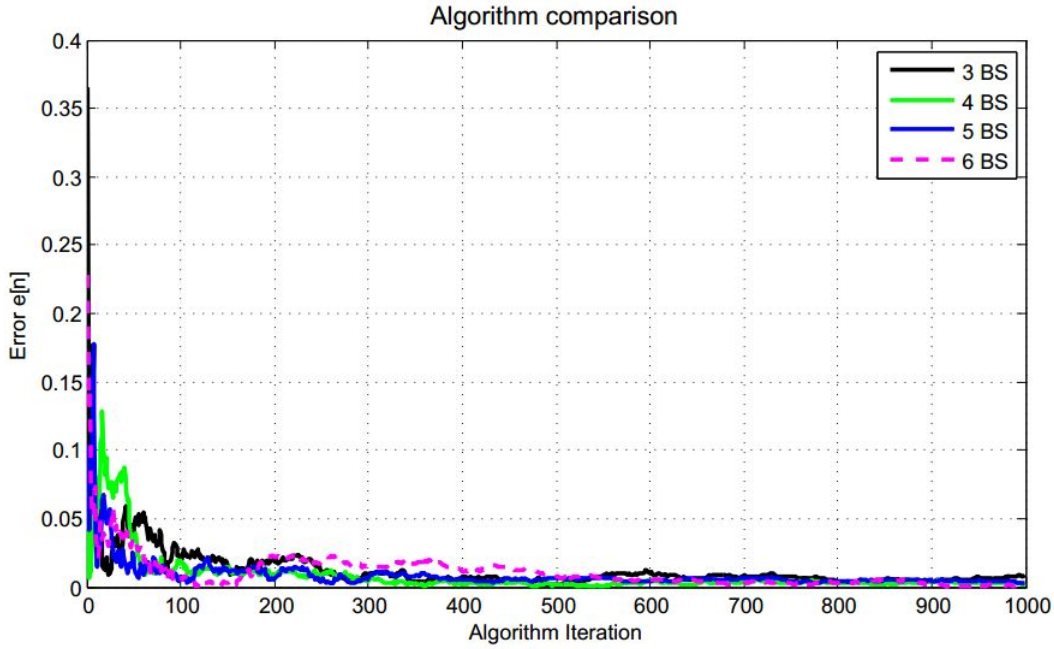

Figure 4.2.5: Comparison for low error

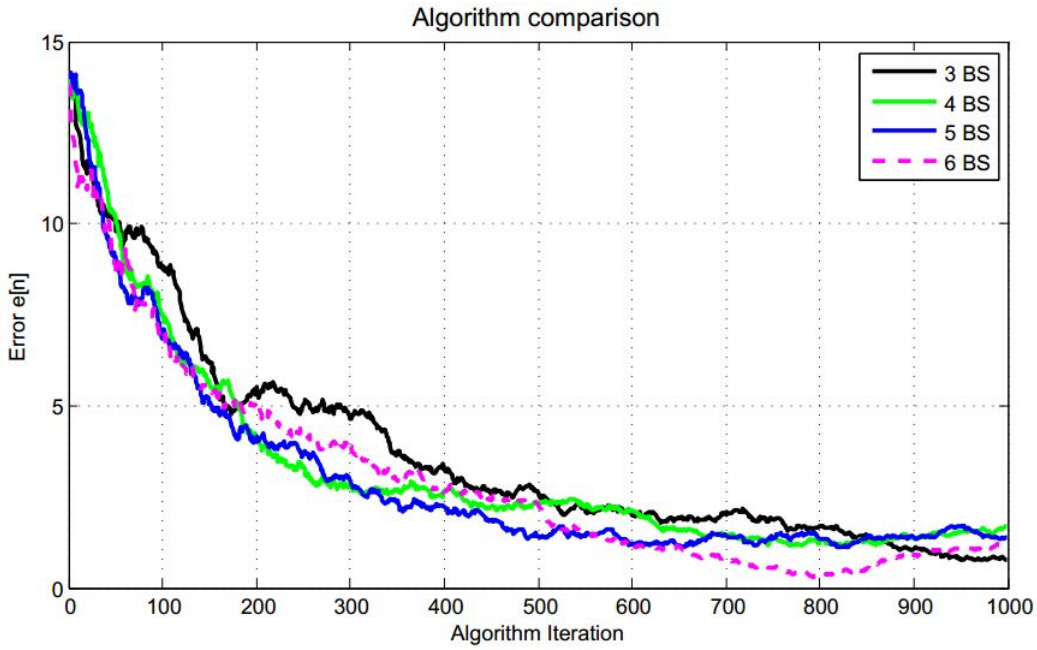

Figure 4.2.6: Comparison for high error

It is noted that the algorithm performs similarly irrespective of how many BS are taken into consideration, both for low error and high error.

The algorithm is then run for the BS environment of Figure 4.2.7 , where all six stations are not equidistant from the origin.

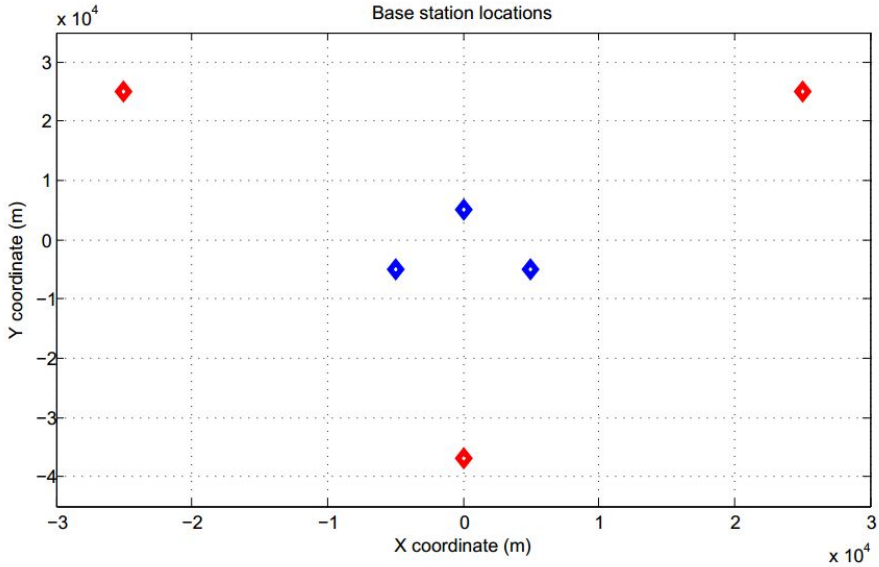

Figure 4.2.7: BS configuration 3

The algorithm is run employing $TDOA$ values from the BS in blue, which are closer to the MS, followed by values involving all six BS for different levels of error.

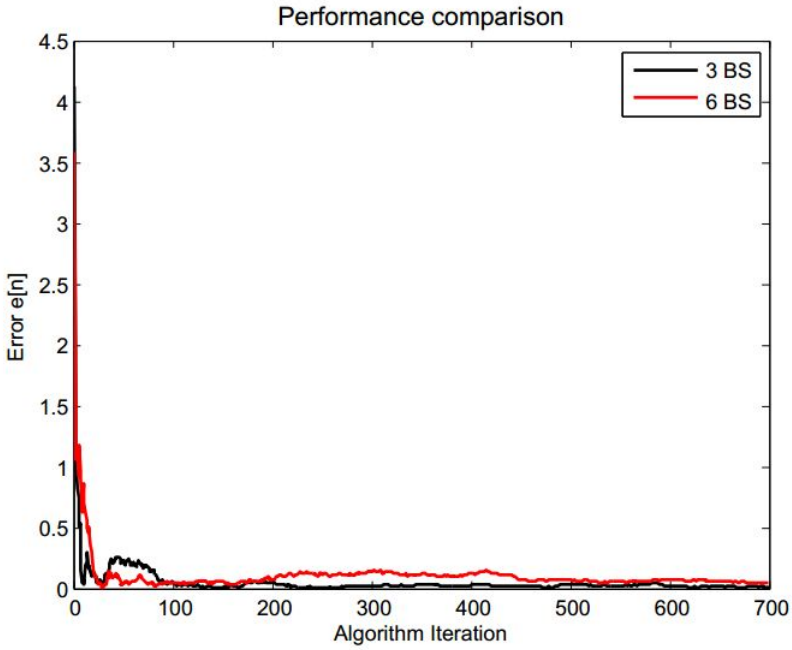

Figure 4.2.8: Comparison for low measurement error

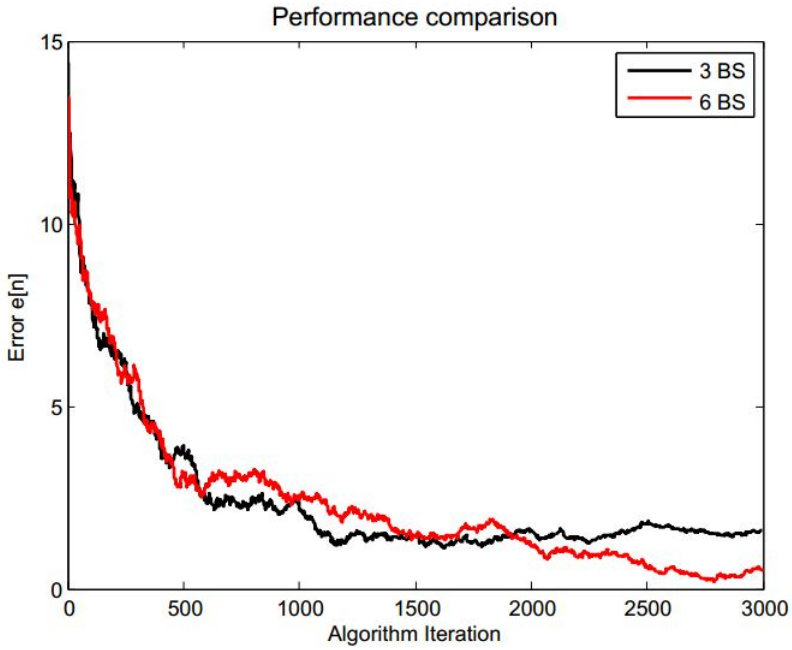

Figure 4.2.9: Comparison for high measurement error

We observe that there is no significant change in algorithm performance by increasing the number of $TDOA$ inputs. Therefore, the algorithm can be run simply by considering the three earliest arrivals (three nearest BS) in a two-dimensional scenario.

4.3 Algorithm simulation for a multipath channel

The algorithm is simulated for a multipath channel in this section. First a pedestrian profile is considered followed by a vehicular profile. The doppler shift depends on the speed of the MS, and the parameters used in this simulation are described in the following table.

S.no	Parameter	Value
1	Pedestrian profile velocity	$1m/s$
2	Pedestrian doppler shift f_d	$0.07Hz$
3	Vehicular velocity	$10m/s$
4	Vehicular doppler shift f_d	$0.7Hz$

Table 4.3: Parameter values 3

The BS configuration employed for the following simulations is shown in Figure 4.3.1.

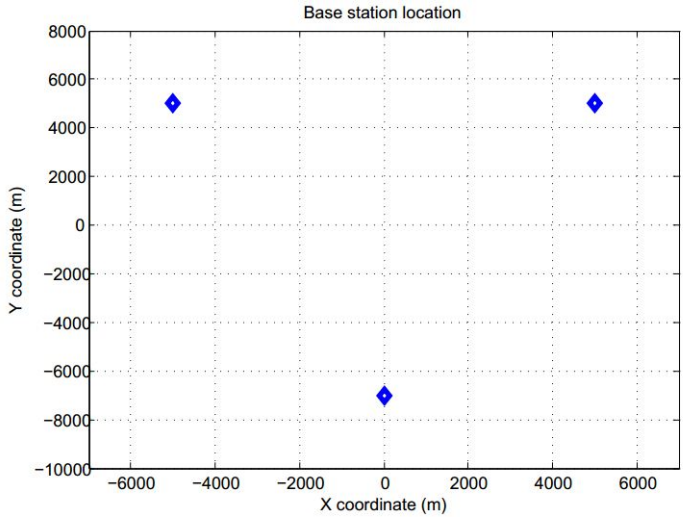

Figure 4.3.1: Rayleigh fading for the pedestrian profile

4.3.1 Pedestrian profile

The PDP for the pedestrian profile is as shown in the following table:

Tap number	Relative Path Power (dB)	Delay (ns)
1	0	0
2	-0.9	200
3	-4.9	800
4	-8.0	1200
5	-7.8	2300
6	-23.9	3700

Table 4.4: Power Delay Profile of a pedestrian channel model

The Rayleigh fading for an MS moving at $1m/s$ is shown in Figure 4.3.2. This was generated using the Jake's method.

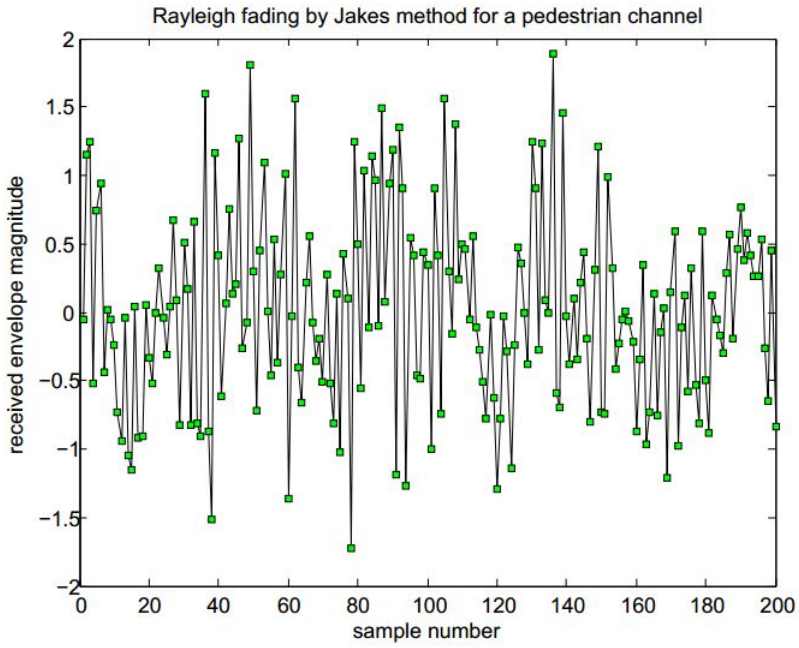

Figure 4.3.2: Rayleigh fading for the pedestrian profile

We deduce the channel impulse response from the PDP values in Table 4.4 and from the fading described in Figure 4.3.2. The following figure depicts an example of the six taps in the impulse response.

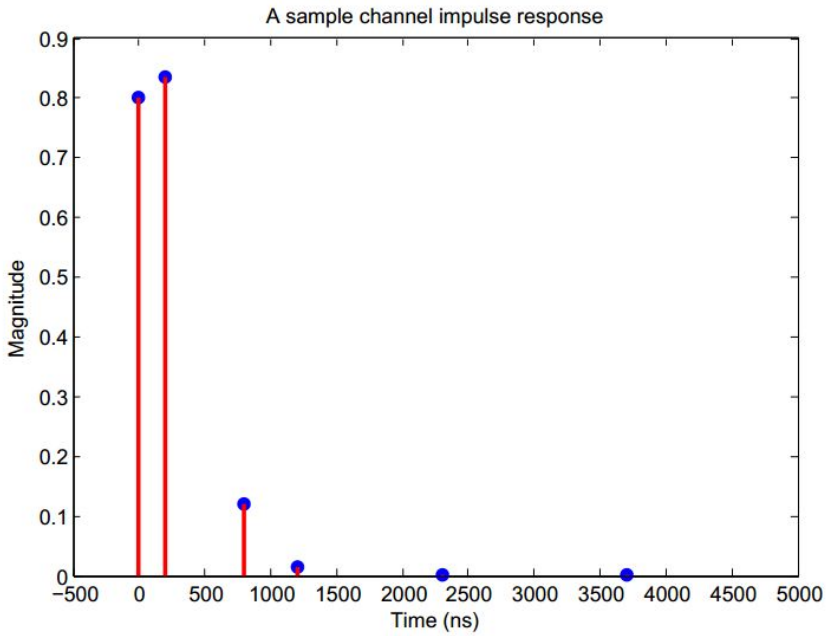

Figure 4.3.3: Channel impulse response for the pedestrian profile

In a real scenario, there is error in both the magnitude as well as the position of the taps. We add these errors, and choose the tap with maximum amplitude in all the BS to obtain $TDOA$ values for the algorithm.

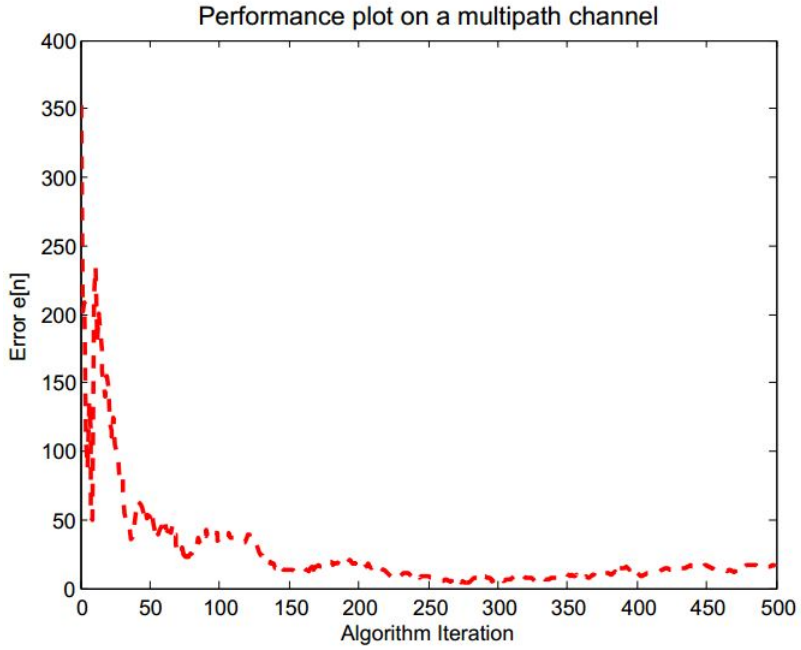

Figure 4.3.4: Algorithm performance for the pedestrian channel

4.3.2 Vehicular profile

The PDP for the vehicular profile is as shown in the following table:

Tap number	Relative Path Power (dB)	Delay (ns)
1	0	0
2	-1	310
3	-9	710
4	-10	1090
5	-15	1730
6	-20	2510

Table 4.5: Power Delay Profile of a vehicular channel model

The Rayleigh fading for an MS moving at $10m/s$ is shown in Figure , generated using the Jake's methid like in the previous channel model.

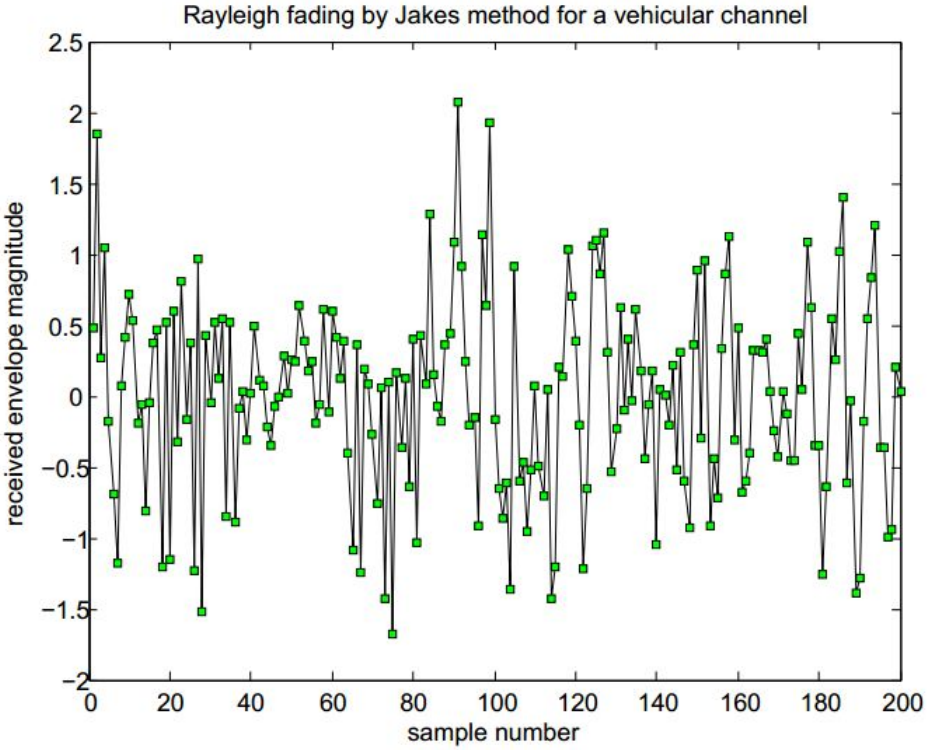

Figure 4.3.5: Rayleigh fading for the vehicular profile

The channel impulse response is depicted in the following figure.

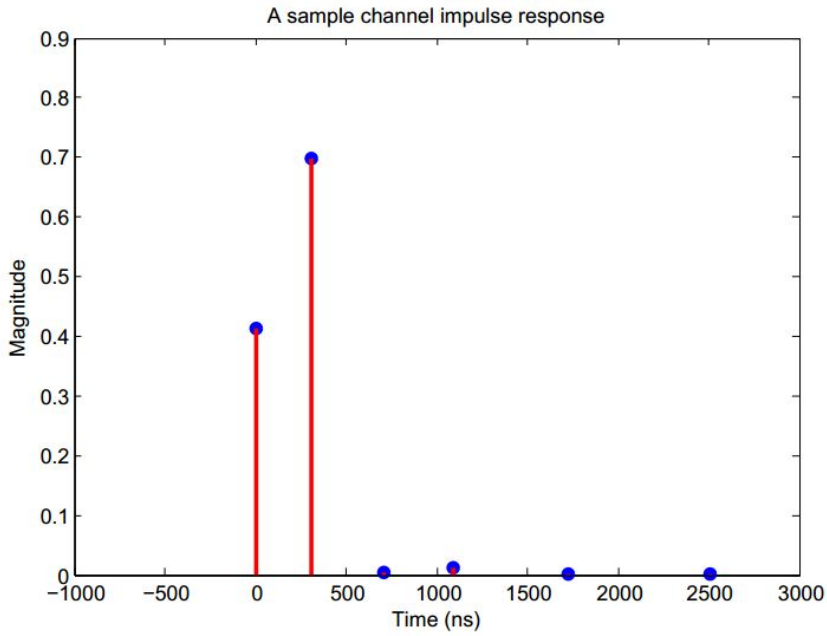

Figure 4.3.6: Channel impulse response for the vehicular profile

We add error to both the amplitude and the position of the taps, and choose the tap with the maximum amplitude in all the BS to obtain the $TDOA$ data.

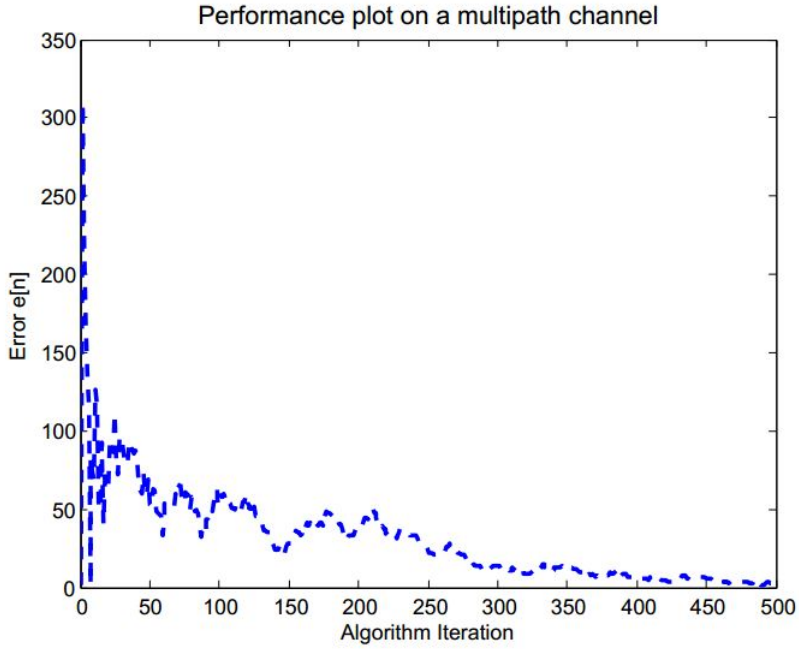

Figure 4.3.7: Algorithm performance for the vehicular channel

From Figures 4.3.4 and 4.3.7, we see that the proposed algorithm converges quite rapidly. Therefore, the algorithm works satisfactorily in case of a multipath channel.

4.4 Conclusions and Future Work

An EKF based localization algorithm based on the multilateration technique is proposed in this thesis that is robust, as seen in section 4.2.1. The algorithm works roughly similarly for any length of measurement input vector as depicted in section 4.2.2, and therefore can be run with minimum data values (three in the two dimensional case). The $TDOA$ values corresponding to the three nearest BS to the MS could be chosen. Performance in an assumed multipath channel is also satisfactory, and is tested for two profiles in section 4.3.

The multipath analysis in this thesis assumes a channel model. The next step could be estimation of the channel, alongwith the recursive EKF algorithm employed here. Also, to obtain $TDOA$ values, the tap with the highest amplitude is chosen. A better selection rule could be employed to determine a better set of $TDOA$ data to ensure faster convergence and reliability. The multilateration technique could be extended to particle filtering as well.

REFERENCES

[1] H.C. Schau and A.Z Robinson , "Passive Source Localization Employing Intersecting Spherical Surfaces from Time-of-Arrival Differences " , IEEE Transactions on Acoustics, Speech and Signal Processing (Volume:35, Issue: 8).

[2] H.C. So and Frankie K. W. Chanc , "A Generalized Subspace Approach for Mobile Positioning With Time-of-Arrival Measurements " , IEEE Transactions on Signal Processing , (Volume:55 , Issue: 10).

[3] Stefan Galler, Waldemar Gerok, Jens Schroeder, Kyandoghere Kyamakya, and Thomas Kaiser , "Combined AOA/TOA UWB localization" , IEEE Transactions on Communications and Information Technologies, 2007. ISCIT '07.

[4] Montse Najar and Josep Videl , "Kalman Tracking based on TDOA for UMTS Mobile location",12th IEEE International Symposium on Personal, Indoor and Mobile Radio Communications, 2001 .

[5] Benjamin Friedlander , "A Passive Localization Algorithm and Its Accuracy Analysis " , IEEE Journal of Oceanic Engineering, Vol. OE-12, No 1, January 1987.

[6] Steven M.Kay , "Fundamentals of Statistical Signal Processing, Volume I: Estimation Theory" , Prentice Hall, 1993.